Rheumatology, 2023, **62**, 3459–3468
https://doi.org/10.1093/rheumatology/kead068
Advance access publication 8 February 2023
Original Article

British Society for Rheumatology RHEUMATOLOGY OXFORD

Basic science

A novel TNFRSF1A mutation associated with TNF-receptor-associated periodic syndrome and its metabolic signature

Joachim D. Steiner [1,2], Andrea Annibal [2], Raymond Laboy[2], Marie Braumann[1], Heike Göbel[3], Valentin Laasch[2], Roman-Ulrich Müller[1,4], Martin R. Späth[1], Adam Antebi[2,4], Torsten Kubacki [1,*]

[1]Department II of Internal Medicine and Center for Molecular Medicine Cologne, Faculty of Medicine and University Hospital Cologne, University of Cologne, Cologne, Germany
[2]Max Planck Institute for Biology of Ageing, Cologne, Germany
[3]Institute of Pathology, University Hospital of Cologne, Cologne, Germany
[4]Cologne Excellence Cluster on Cellular Stress Responses in Aging-Associated Diseases (CECAD), University of Cologne, Cologne, Germany

*Correspondence to: Torsten Kubacki, University Hospital of Cologne, Kerpener Str. 37, 50937 Cologne, Germany. E-mail: torsten.kubacki@uk-koeln.de

Abstract

Objective: We describe a family with a novel mutation in the TNF Receptor Superfamily Member 1A (*TNFRSF1A*) gene causing TNF receptor–associated periodic syndrome (TRAPS) with renal AA amyloidosis.

Methods: Case series of affected family members. We further investigated the plasma metabolome of these patients in comparison with healthy controls using mass spectrometry.

Results: In all symptomatic family members, we detected the previously undescribed variant c.332A>G (p.Q111R) in the *TNFRSF1A* gene. Canakinumab proved an effective treatment option leading to remission in all treated patients. One patient with suspected renal amyloidosis showed near normalization of proteinuria under treatment. Analysis of the metabolome revealed 31 metabolic compounds to be upregulated and 35 compounds to be downregulated compared with healthy controls. The most dysregulated metabolites belonged to pathways identified as arginine biosynthesis, phenylalanine, tyrosine and tryptophan biosynthesis, and cysteine and methionine metabolism. Interestingly, the metabolic changes observed in all three TRAPS patients seemed independent of treatment with canakinumab and subsequent remission.

Conclusion: We present a novel mutation in the *TNFRSF1A* gene associated with amyloidosis. Canakinumab is an effective treatment for individuals with this new likely pathogenic variant. Alterations in the metabolome were most prominent in the pathways related to arginine biosynthesis, tryptophan metabolism, and metabolism of cysteine and methionine, and seemed to be unaffected by treatment with canakinumab. Further investigation is needed to determine the role of these metabolomic changes in the pathophysiology of TRAPS.

Received: 10 November 2022. **Accepted:** 29 January 2023

Graphical abstract

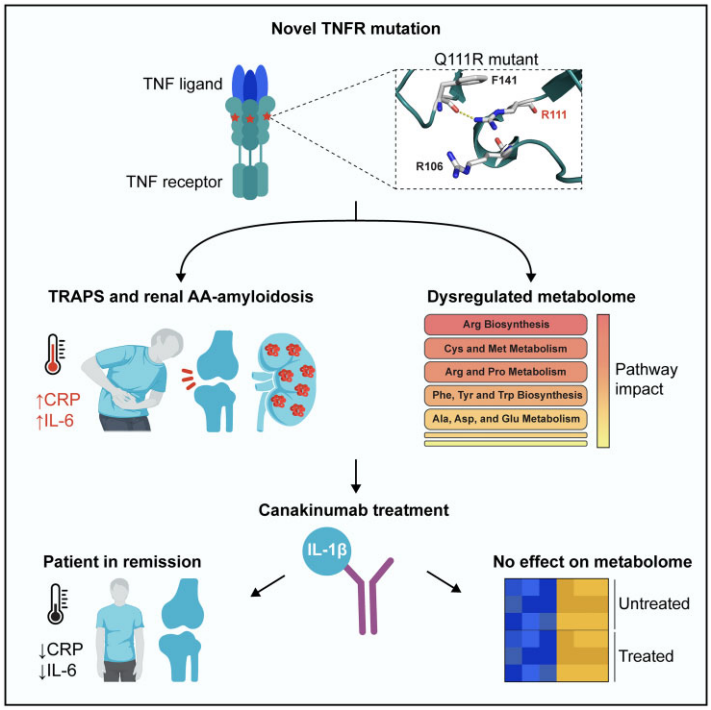

Keywords: TRAPS, amyloidosis, canakinumab, metabolomics, kidney, kynurenine, tryptophan, methionine, choline

Rheumatology key messages

- c.332A>G (p.Q111R) is a novel pathological mutation within the *TNFRSF1A* gene that causes AA amyloidosis.
- Early renal amyloidosis is potentially reversible upon adequate inflammation control with canakinumab.
- TRAPS patients show dysregulated plasmametabolome with marked changes in arginine, tryptophan and methionine metabolism regardless of disease activity.

Introduction

TNF receptor–associated periodic syndrome (TRAPS) is an autosomal dominantly inherited periodic fever syndrome. Heterozygous pathogenic variants in the TNF Receptor Superfamily Member 1A (*TNFRSF1A*) gene cause TRAPS, which leads to dysregulation of the innate immune system and subsequent systemic inflammation [1]. It is clinically characterized by prolonged episodes of fever, arthralgia, myalgia, abdominal pain and erythematous rash [2]. As a rare disease, the prevalence is estimated to be around one case per million people [3, 4].

Here we report a new mutation in the *TNFRSF1A* gene in a Caucasian family, which is associated with TRAPS and AA amyloidosis. We also evaluate its response to treatment with the IL-1β inhibitor canakinumab. Pathologic variants in the *TNFRSF1A* gene disrupt the folding of the protein, which affects protein structure and expression on the cell surface and results in subsequent intracellular accumulation. This leads to increased endoplasmic stress, upregulation of the unfolded protein response, and increased production of reactive oxygen species (ROS) in mitochondria [5] resulting in enhanced activation of NF-κB and MAPK signalling and thus an increase in levels of pro-inflammatory cytokines (e.g. IL-1β, TNF, IL-6) [5–7]. Persistent inflammation has been shown to have a strong impact on metabolic patterns. On the one hand, stimulated immune cells adapt their metabolism to provide sufficient energy for the proliferation and production of pro-inflammatory mediators. On the other hand, inflammatory responses are subject to regulation by metabolic pathway activity. Based on these aspects, gaining more insights into changes in metabolism in the context of TRAPS may facilitate the identification of both markers of disease activity and potential therapeutic targets. Consequently, we decided to use a mass spectrometry approach to study the changes in metabolic processes in three affected family members compared with age- and sex-matched healthy controls.

Methods

Genetic testing and *in silico* analyses of mutation

Next-generation sequencing was performed by SYNLAB Mannheim (https://www.synlab.de/lab/mannheim-genetik). We used the PolyPhen-2 web-software [8] and PROVEAN [9] for pathogenicity predictions of the mutation. Crystal

structure 1FT4 (10.1073/pnas.211178398) [10] obtained from the Protein Data Bank (www.rcsb.org) was modelled in PyMOL (v2.5.4) [11]. Subsequently, the Q111R mutation was generated to predict changes in the interactions between residues.

Metabolite extraction from plasma

Heparinized whole blood was obtained from study participants after written informed consent was given according to approval by the ethics committee (vote 12–240), University of Cologne, Cologne, Germany. The study is registered at the German Clinical Trials Registry under the ID: DRKS00010534. Plasma protein concentration was measured using a bicinchoninic acid (BCA) kit (Thermo Fisher Scientific, Bremen, Germany). Metabolites were extracted using the Folch Method as described previously [12]. Briefly, 200 µl of chloroform and 150 µl of methanol were added to the plasma. Samples were shaken for 1 h at 4°C, followed by centrifugation at 3000 r.c.f. for 10 min at 4°C.

A volume of sample corresponding to 100 µg protein was collected and dried out using a speed vac. The samples were reconstituted in 10 µl of acetonitrile, and 5 µl was injected into the MS instrument.

Untargeted metabolomics

Analytes were separated using a Ultra-High-Performance Liquid Chromatography (UHPLC) system (Vanquish, Thermo Fisher Scientific, Bremen, Germany) coupled to an High-Resolution Accurate-Mass (HRAM) mass spectrometer (Q-Exactive Plus, Thermo Fisher Scientific GmbH, Bremen, Germany) as described previously [13]. Briefly, 2 µl of sample extract were injected into an X Select HSS T3 XP column, 100 Å, 2.5 µm, 2.1 mm × 100 mm (Waters), using a binary system comprised of two solutions, A: water with 0.1% formic acid, B: acetonitrile with 0.1% formic acid, operating at a flow rate of 0.1 ml/min and a column temperature kept at 30°C. Gradient elution was conducted as follows: isocratic step at 0.1% eluent B for 0.5 min, gradient increase up to 2% eluent B in 2 min, then increased up to 30% eluent B in 6 min and to 95% eluent B in 7 min, isocratic step at 95% eluent B for 2 min. The gradient was decreased to 0.1% eluent B in 3 min and held at 0.1% eluent B for 5 min. Mass spectra were recorded from 100–800 m/z at a mass resolution of 70 000 at m/z 400 in both positive and negative ion modes using data-dependent acquisition. Tandem mass spectra were acquired by performing collision-induced dissociation (CID). Sample injection order was randomized to minimize the effect of instrumental signal drift. MS data analysis was performed using Xcalibur software 4.0.

Compound identification and quantification

Metabolite search was performed using the online databases Compound Discoverer 2.0 and mzCloud, considering precursor ions with a deviation <5 p.p.m., 0.5 min maximum retention time shift, minimum peak intensity 10^5, intensity tolerance 10, FT fragment mass tolerance 0.0025 Da, group covariance <30%, *P*-value <0.05 and area Max ≥10 000. Metabolites were considered to be correctly identified when at least two specific fragments were found in the MS2 spectra. Quantification was performed using Trace finder 4.1, genesis detection algorithm, nearest RT, S/N threshold 8, min peak height (S/N) equal to 3, peak S/N cut-off 2.00, valley rise 2%, valley S/N 1.10. Relative quantification was obtained by dividing the area of individual metabolites to spiked internal standards (leucine enkephalin, myristic acid and cysteamine sodium salt).

Statistical analyses

Quantified metabolites were analyzed using the inbuilt tools of the MetaboAnalyst platform (metaboanalyst.ca) [14]. Changes in single metabolites were classified as significant when log2FC >0.5 and *t*-test returned both $P < 0.05$ and false discovery rate <0.05 (Supplementary Table S1, available at *Rheumatology* online). The quantitative enrichment analysis and pathway analysis modules were used for pathway analyses (Supplementary Tables S2 and S3, available at *Rheumatology* online).

Measurements of inflammatory markers

CRP was determined by the CRP Latex Test Gen. 3, a particle-enhanced immunoturbidimetry (Roche Diagnostics®) with the Cobas C702 analyser system. IL-6 was determined by the Elecsys IL-6 (Roche Diagnostics®), a sandwich immunoassay, using the Cobas E801 analyser system.

Results

A 44-year-old man (patient 1) presented to our hospital with abdominal pain, highly elevated inflammation parameters and chronic kidney disease with severe proteinuria at stage G5A3 according to the Kidney Disease: Improving Global Outcomes (KDIGO) (Fig. 1A). Kidney biopsy showed severe AA amyloidosis (Fig. 2). Patient history revealed recurrent attacks of abdominal pain with fever and elevation of inflammatory markers such as CRP that had first occurred at the age of 16 years. He also reported that his father, aunt, sister and daughter had similar problems (Fig. 1B).

His 19-year-old daughter (patient 2) disclosed that she had had recurrent episodes of abdominal pain with a fever of up to 38.5°C since she was 11 years old (Fig. 1A and B). The attacks lasted >14 days and occurred three to five times a year. Due to the recurrent abdominal pain attacks, she had already had an appendectomy at the age of 15 years and had undergone a diagnostic laparoscopy, where endometriosis was suspected, but only signs of unspecific peritonitis were evident. She denied skin rashes during the attacks. At the time of her presentation to our department, she showed highly elevated CRP levels (263 mg/dl) but only reported mild abdominal pain when asked. Kidney function was normal, and proteinuria was within normal range. The 46-year-old sister of patient 1 (patient 3) also presented with a history of recurrent abdominal pain and fever at 6- to 8-week intervals since the age of 12 years (Fig. 1A and B). She also reported suffering from cervical lymphadenopathy and arthralgia during the attacks. On presentation, she showed mildly impaired kidney function (estimated glomerular filtration rate 63 ml/min/1.73 m^2) and proteinuria of 2000 mg/g creatinine (albuminuria 1500 mg/g creatinine), strongly suggesting early renal AA amyloidosis.

All five symptomatic family members underwent genetic testing that revealed the *TNFRSF1A* variant c.332A>G (p.Q111R) (Fig. 1C). To our knowledge, this missense variant has not yet been reported in the literature or the infevers database [15, 16]. *In silico* analyses of the mutation by PolyPhen-2 software [8] and Provean [9] classified the mutation as probably damaging (score: 0.999) and deleterious (Provean-

A

		Patient 1	Patient 2	Patient 3
Patient characteristics	Gender	M	F	F
	Age (y)	45	19	47
	Age at onset (y)	16	11	12
	Symptoms	abdominal pain; fever; arthralgia	abdominal pain; fever	abdominal pain; fever; lymphadenopathy; arthralgia
	Attack duration (d)	> 14	> 14	> 14
	Histology	Renal AA amyloidosis	N/A	N/A
Medical treatment	First 6 months	Canakinumab 150 mg every 4 weeks	Canakinumab 150 mg once at first visit	Canakinumab 150 mg every 4 weeks
Selected laboratory parameters at initial presentation	CRP (mg/l)	89	263	65
	SAA (mg/dl)	78.9	155	74
	Creatinine (mg/dl)	4.9	0.74	1.1
	eGFR (ml/min)	13	100	63
	Albuminuria (mg/g creatinine)	4367	4	1574
Selected laboratory parameters at follow-up presentation	CRP (mg/l)	2.1	4.7	0.9
	SAA (mg/dl)	0.86	0.39	0.56
	Creatinine (mg/dl)	6.5	0.83	1.2
	eGFR (ml/min)	14	90	58
	Albuminuria (mg/g creatinine)	3000	4	175

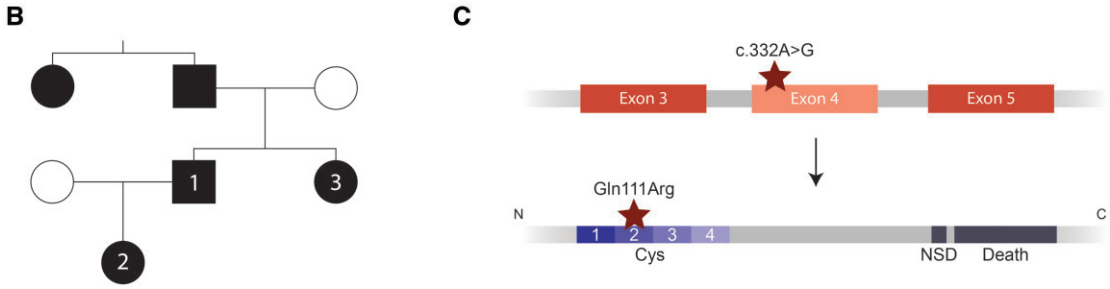

Figure 1. Three patients presenting with a novel TRAPS causing mutation. (**A**) Patient characteristics and selected laboratory markers at initial presentation and at follow-up visit. SAA: Serum Amyloid A; eGFR: estimated glomerular filtration rate, estimated using the full age spectrum (FAS) equation). (**B**) Pedigree of patient family. Patients denoted as 1, 2 and 3, respectively, presented to our hospital. (**C**) Schematic representation of the mutation in exon 4 of the *TNFRSF1A* gene present in all three patients and of the ensuing amino acid substitution at protein level. Cys: cysteine-rich domain; NSD: N-SMASE activation domain; Death: death domain; TRAPS: TNF receptor–associated periodic syndrome; *TNFRSF1A*: TNF Receptor Superfamily Member 1A gene

Score: –3.541), respectively. *In silico* analysis via the PyMOL software [11] and the Project HOPE server [17] was performed to obtain three-dimensional representations of the protein (Fig. 3A). Modelling of the mutation revealed that the mutant residue (Q111R) is larger than the wild-type residue and is positively charged, whereas the wild-type is neutral. Unlike wild-type (Fig. 3B), mutant residues cannot form hydrogen bonds with the backbone carbonyl group R106 likely affecting the proper folding of this domain (Fig. 3C). The mutation is located in the cysteine-rich domain 2 of the protein's extracellular domain, where most TRAPS-causing mutations are reported (Fig. 1C) [5].

Taking into account the typical clinical picture, the histological evidence of renal AA amyloidosis, the detection of a mutation in the *TNFRSF1A* gene and the fact that the mutation was found in the extracellular domain of TNR1A, the diagnosis of TRAPS was made.

All patients received the IL-1β inhibitor canakinumab for treatment, and all responded with normalization of inflammatory parameters and clinical remission. Fig. 1A shows the clinical characteristics and laboratory results of all patients. Notably, patient 3 showed a marked decrease in proteinuria during treatment with canakinumab, which we interpret as an improvement in suspected early renal AA amyloidosis. While the pro-inflammatory and pathophysiological changes in TNFα signalling have been well described, the impact of these mutations on metabolism has not been sufficiently studied to date [7, 18]. Thus, we used mass spectrometry to test metabolomic changes in the patients.

Fig. 4A shows a heatmap of metabolic changes in the plasma of our three patients during disease flares and during remission (defined by the absence of clinical symptoms and normal levels of CRP as well as IL-6; Fig. 5C) compared with age- and sex-matched healthy controls. We found 31 metabolites upregulated and 35 compounds downregulated (Supplementary Table S1, available at *Rheumatology* online).

Intriguingly, these metabolic changes seemed to be independent of disease activity (Figs 4A and 5A).

Among the significantly upregulated metabolites, we identified hypoxanthine, kynurenine, phenylalanine and choline (Fig. 4B), while tryptophan, arginine, tyrosine and methionine were found to be among the significantly downregulated metabolites (Fig. 4C).

Quantitative enrichment analyses revealed that arginine biosynthesis and tryptophan metabolism were among the most enriched pathways according to the Kyoto Encyclopedia of Genes and Genomes (KEGG) library (Fig. 4D, Supplementary Table S2, available at *Rheumatology* online).

Sparse partial least-squares discriminant analysis (sPLS-DA) confirmed a distinct signature for all patients compared with healthy controls, while no differences were evident concerning disease activity (Fig. 4E). Notably, arginine biosynthesis and biosynthesis of phenylalanine, tyrosine and tryptophan also scored high when quantifying the impact of KEGG pathways using pathway enrichment analyses. In addition, cysteine and methionine metabolism emerged as another impactful pathway (Fig. 5B, Supplementary Table S3, available at *Rheumatology* online).

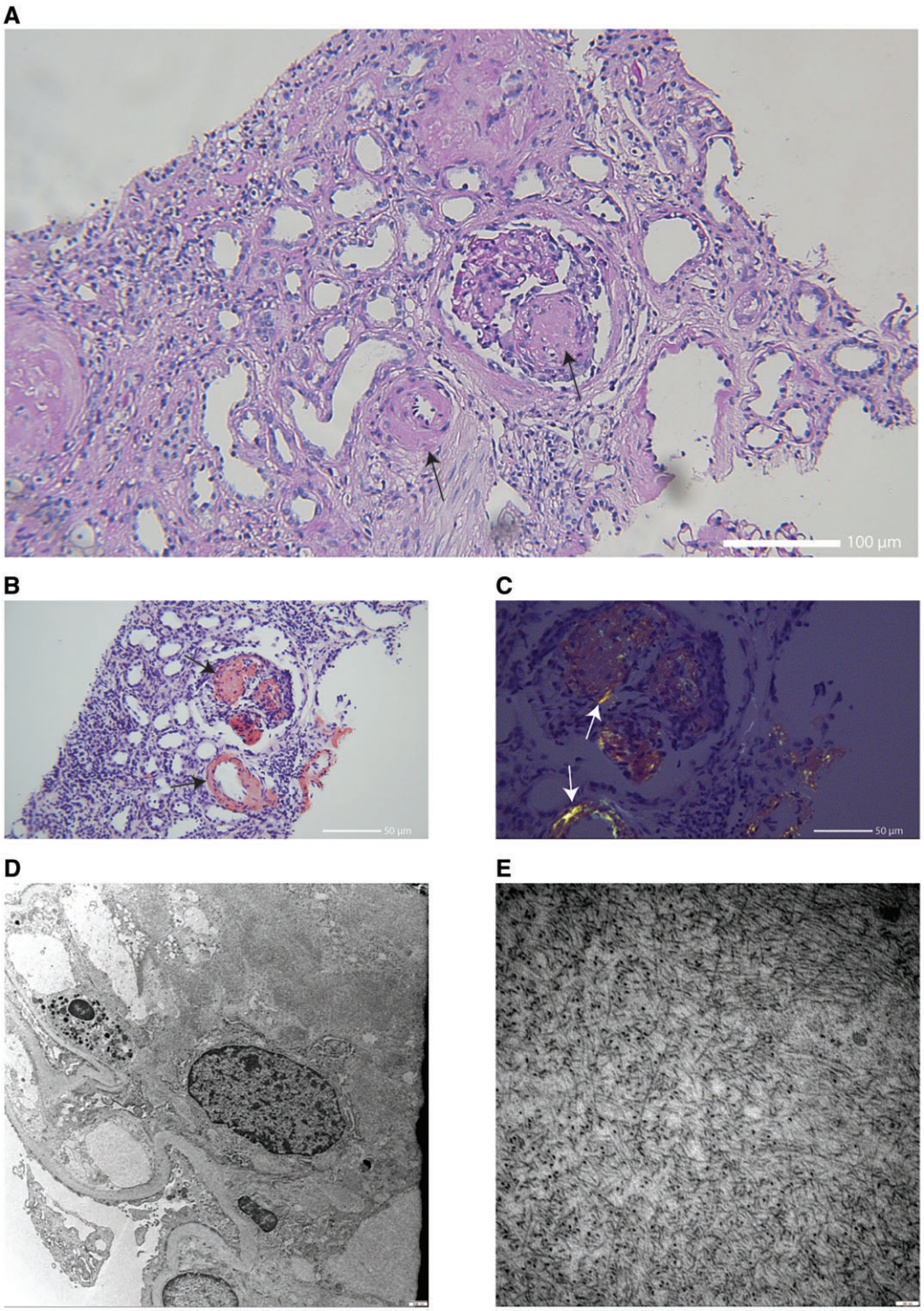

Figure 2. Histology of the kidney of patient 1 reveals renal AA amyloidosis. (**A**) Light microscopy of the kidney shows deposits of amorphous material in glomeruli and arterioles (marked by black arrows). Periodic acid–Schiff (PAS) stain. (**B**) Congo red staining identifies deposits as amyloid (marked by black arrows). (**C**) Polarized light microscopy identifies deposits as amyloid (marked by white arrows). (**D**) Electron microscopy overview (magnification 2100×) of a glomerulus shows cloudy structures. (**E**) Higher magnification (46400×) of (D) shows cloudy structures are identifiable as amyloid fibrils

Discussion

We present a novel *TNFRSF1A* variant c.332A>G (p.Q111R) causing TRAPS in affected patients. We observed a remarkable response with normalization of inflammatory parameters in all three patients upon initiating treatment with the IL-1β antibody canakinumab. Furthermore, we interpret the near normalization of proteinuria in patient 3 as regressive amyloidosis of the kidney. This is in line with findings that early intervention targeting the IL-1 pathway can stop or improve the course of renal amyloidosis in patients with FMF [19].

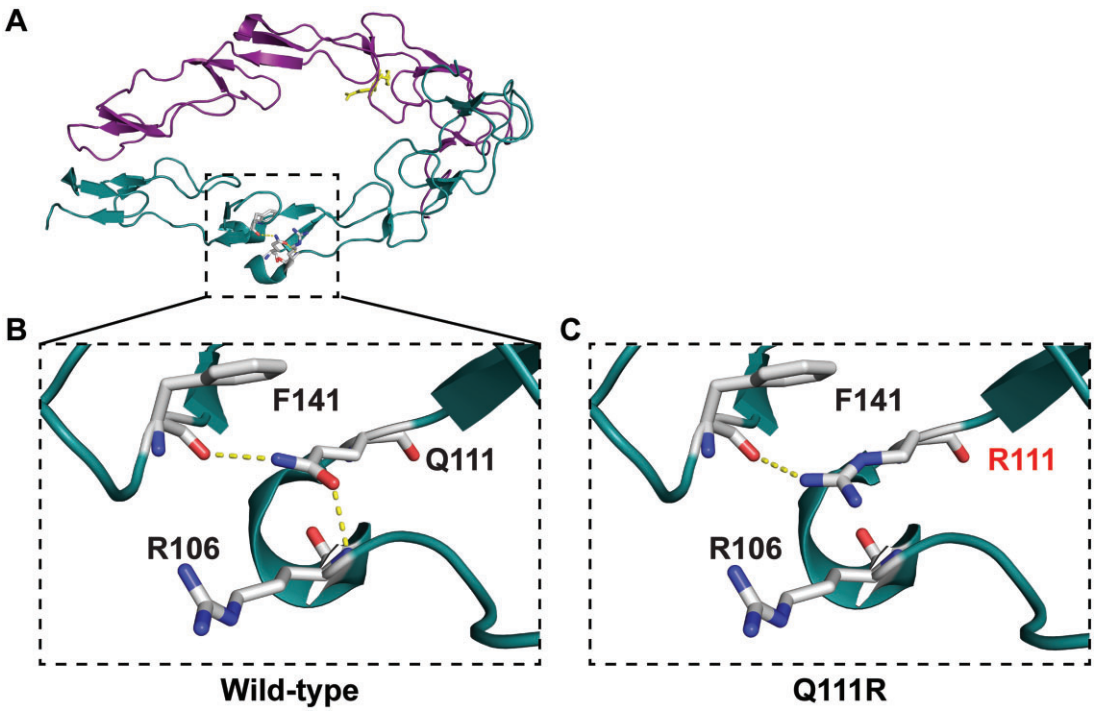

Figure 3. 3D model of TNR1A reveals disruption of hydrogen bonds. (**A**) Cartoon representation of dimeric TNR1A (PDB 1FT4); one monomer is coloured in deep teal, and the second monomer is in deep purple. (**B**) Magnification of the region containing Q111 and neighbouring interacting residues R106 and F141 shown in sticks. Carbons are colour-coded in grey, nitrogen in blue and oxygen in red. Hydrogen bonds are depicted as yellow dashed lines. (**C**) Q111R mutation disrupts the interaction with the backbone carbonyl group R106, likely affecting the proper folding of this domain. Images were generated with PyMOL (v2.5.4) [1]. TNR1A: TNF Receptor 1A

In contrast to the effects of canakinumab on inflammation, the metabolomic signature did not correlate with disease activity. This can be considered analogous to observations from TRAPS patients, where blocking the action of pro-inflammatory cytokines associated with TRAPS (e.g. IL-1, TNF) could improve clinical symptoms but did not affect the underlying activation of intracellular inflammatory signalling pathways [20].

Many affected pathways, such as arginine biosynthesis (Fig. 5D) and tryptophan metabolism, have been described as dysregulated in inflammation (reviewed in Ref. [21]). In humans, Indoleamine-2,3-dioxygenase (IDO) catabolizes the initial steps of a series of reactions leading to the conversion of tryptophan to kynurenine. These reactions seem activated in inflammation, with the tryptophan/kynurenine ratio being suggested as a marker for infectious diseases such as COVID-19 [22, 23]). Interestingly, it has been shown that pro-inflammatory cytokines may prime macrophages and dendritic cells to express IDO and release ROS, leading to the conversion of tryptophan to kynurenine and inhibiting the conversion of phenylalanine to tyrosine, respectively (Fig. 5E) [24, 25].

In addition, activated macrophages have also been studied regarding choline metabolism, which was enriched in all patients (Fig. 4B). For example, it has been shown that activated murine macrophages can enhance choline uptake, increasing IL-1 and IL-18 production [26]. Furthermore, dietary supplementation of choline in mice led to upregulation of the scavenger factor CD36 [27]. Murine macrophages deficient in CD36 have been shown to display downregulation of pro-inflammatory cytokines and reduced oxidative stress [28, 29]. The notion that increased choline levels contribute to the disease phenotype is supported by findings in a mouse model of Muckle–Wells syndrome, a different periodic fever syndrome. Here the absence of choline led to a reduction in disease severity [26]. In humans, both beneficial and harmful effects of choline have been described. A study analysing the metabolic profile changes in the plasma of patients diagnosed with inflammatory RA found choline to be increased [30]. Conversely, choline has been described to attenuate immune activity in asthma patients and to ameliorate cardiovascular damage by inhibiting the inflammatory response in rats [31, 32].

It is noteworthy that choline is linked to methionine metabolism, which we observed to be among the most impactful pathways to be dysregulated (Fig. 5B and F). Betaine, a choline derivative, is required to convert homocysteine to methionine [33]. Indeed, we noted upregulation of homocysteine while methionine appeared downregulated (Fig. 4C, Supplementary Table S1, available at *Rheumatology* online). In line with this, we also detected the downregulation of S-adenosyl-methionine which is produced in the conversion of methionine to homocysteine (Fig. 5F) [34]. Homocysteine synthesis from methionine also leads to adenosine production, which is subsequently converted to hypoxanthine (Fig. 5F) [35]. Hypoxanthine can then be oxidized to xanthine and uric acid in ensuing reactions (Fig. 5F). Of note we found hypoxanthine to be highly enriched while both adenosine and xanthine were slightly decreased; however, not to a level of log2FC >0.5. In the context of cancer, increased production of purines from hypoxanthine has been described to suppress immune function through downregulation of IL-1β in the tumour microenvironment [36]. We interpret the enrichment of hypoxanthine in our data to be a reflection of TRAPS-induced hyperactivation of immune cells.

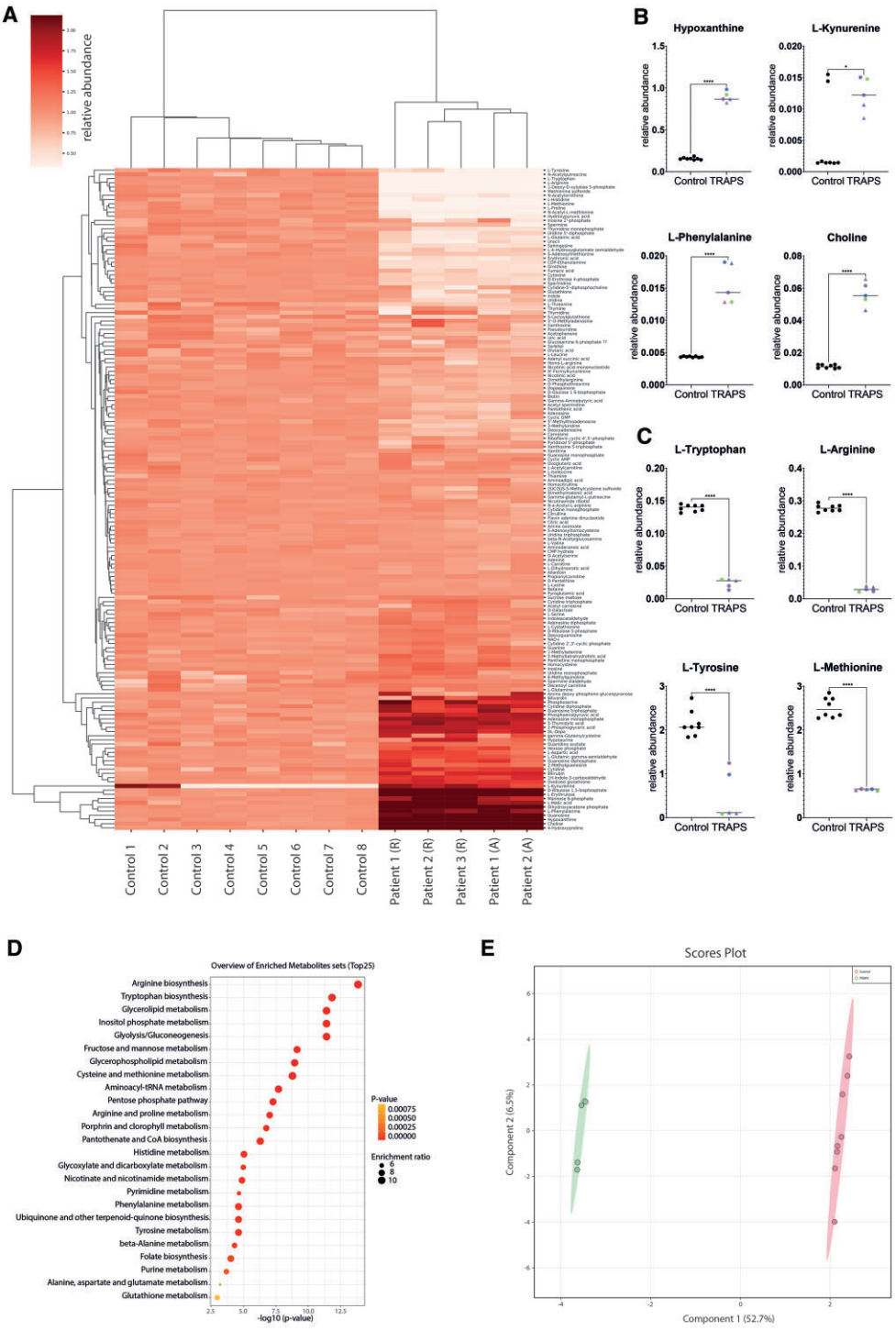

Figure 4. Plasma metabolome of TRAPS patients is dysregulated compared with healthy controls. (**A**) Untargeted metabolomic analysis of three patients compared with eight age- and sex-matched healthy controls. For patients 1 and 2, samples obtained during active disease flares (A) and during remission (R) were analyzed. Heat map depicting log2-transformed abundance of metabolites (normalized to internal standard) relative to the average of controls (listed in Supplementary Table S1, available at *Rheumatology* online). Metabolites and samples were hierarchically clustered using Euclidean metrics. (**B**) Relative abundance of hypoxanthine, L-kynurenine, L-phenylalanine and choline in TRAPS patients compared with healthy controls. Blue symbols denote patient 1, purple symbols patient 2 and green symbols patient 3. Circles denote disease in remission while triangles denote active disease. Significance was assessed using unpaired *t*-test: $^{****}P < 0.0001$ and $^{*}P < 0.05$. (**C**) Relative abundance of L-tryptophan, L-arginine, L-tyrosine and L-methionine in TRAPS patients compared with healthy controls. Blue symbols denote patient 1, purple symbols patient 2 and green symbols patient 3. Circles denote disease in remission while triangles denote active disease. Significance was assessed using unpaired *t*-test: $^{****}P < 0.0001$. (**D**) Quantitative enrichment analysis obtained by uploading all quantified metabolites to MetaboAnalyst (https://www.metaboanalyst.ca) [2] in the three patients compared with healthy controls. Only pathways featuring at least five entries were considered. KEGG pathways containing 84 metabolite sets (KEGG, October 2019) were selected. Detailed parameters are shown in Supplementary Table S2, available at *Rheumatology* online. (**E**) Sparse partial least squared-discriminant analysis (sPLS-DA) scores of the untargeted metabolomic features of all five conditions compared with healthy controls obtained from MetaboAnalyst (https://www.metaboanalyst.ca) [2]. Component 1, x-axis; Component 2, y-axis. Both components are comprised of 10 features each. In the score plot, ellipses correspond to the 95% confidence region. TRAPS: TNF receptor–associated periodic syndrome; KEGG: Kyoto Encyclopedia of Genes and Genomes

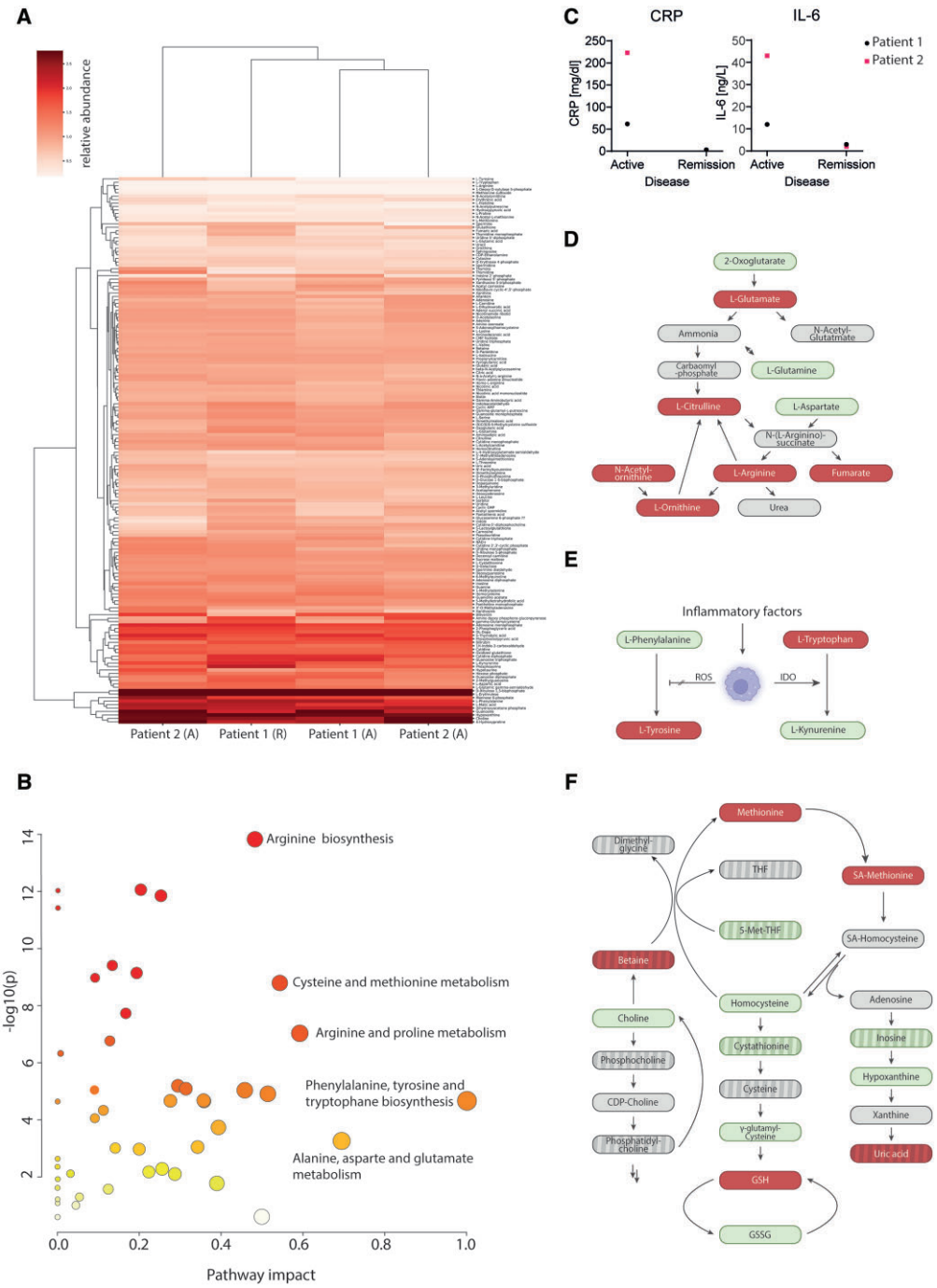

Figure 5. Metabolome of TRAPS patients is independent of disease activity. (**A**) Untargeted metabolomic analysis of patients 1 and 2 during active disease flares (A) and during remission (R). Heat map depicting log2-transformed abundance of metabolites (normalized to internal standard) relative to the average of controls (listed in Supplementary Table S1, available at *Rheumatology* online). Metabolites and samples were hierarchically clustered using Euclidean metrics. (**B**) Pathway analysis was obtained by uploading all quantified metabolites to MetaboAnalyst (https://www.metaboanalyst.ca) [2] in the three patients compared with healthy controls. Only pathways featuring at least five entries were considered. KEGG pathways containing 84 metabolite sets (KEGG, October 2019) were selected. Pathways with the highest impact scores were annotated. Detailed parameters are shown in Supplementary Table S3, available at *Rheumatology* online. (**C**) Inflammatory markers measured during active disease and during remission. Serum levels of CRP were measured using particle-enhanced immunoturbidimetry and levels of IL-6 were determined by the Elecsys IL-6 (Roche Diagnostics®), a sandwich immunoassay, using the Cobas E801 analyser system. (**D**) Schematic representation of the arginine biosynthesis pathway as considered for the pathway analysis in (B). Red rectangles denote metabolites significantly downregulated, grey rectangles denote metabolites not significantly changed and green rectangles denote metabolites significantly upregulated when comparing patients with healthy controls. (**E**) Schematic representation of basic mechanisms by which monocytes/macrophages/dendritic cells can influence selected pathways. ROS: reactive oxygen species; IDO: Indoleamine-2,3-dioxygenase 1. Modified from Ref. [3]. (**F**) Schematic representation of the homocysteine/methionine pathway and its interplay with choline and hypoxanthine metabolism as well as biosynthesis of GSH. Red and green rectangles denote metabolites significantly upregulated and downregulated, respectively. Hatched red rectangles and hatched green denote metabolites significantly upregulated and downregulated, respectively, but failing to reach log2FC >0.5. Grey rectangles denote metabolites not significantly changed when comparing patients with healthy controls. Hatched grey rectangles denote metabolites not measured in our dataset. SA methionine: S-adenosylmethionine; SA-homocysteine: S-adenosylhomocysteine; THF: tetrahydrofolic acid; 5-Met-THF: 5-methyltetrahydrofolic acid; CDP-Choline: cytidine-5′-diphosphocholine; GSH: glutathione; GSSG: oxidized glutathione. Adapted from Refs. [4–6]. TRAPS: TNF receptor–associated periodic syndrome; KEGG: Kyoto Encyclopedia of Genes and Genomes

Hyperhomocysteinemia has been well-described for cardiovascular diseases and RA [37, 38]. In addition, homocysteine has also been shown to drive inflammation through macrophage activation [33]. In microglia, resident brain macrophages, homocysteine leads to activation and subsequent release of inflammatory factors such as TNF-α and IL-6 [39].

All of these changes in metabolite abundance can be observed in the context of oxidative stress. We found oxidized glutathione (GSSG) to be significantly increased and reduced glutathione (GSH) to be significantly decreased, yielding an increased ratio indicative of oxidative stress (Supplementary Table S1, available at *Rheumatology* online Fig. 5F) [40]. Furthermore, increased ROS production—the cause of oxidative stress—has been shown in TRAPS patients independent of disease activity [6]. Thus, we speculate that the overactivation of macrophages in the context of oxidative stress might be one of the mechanisms underlying the observed metabolic changes.

However, further mechanistic studies are needed to elucidate why changes in the metabolome consistent with inflammation do not appear to correlate with clinical symptoms or laboratory parameters of disease activity. This is particularly striking since after treatment of 20 TRAPS patients with canakinumab, many genes relevant to disease pathogenesis moved towards levels seen in the healthy volunteers [41]. Our findings imply that the metabolic changes are not conclusively explained by the phenotypic pro-inflammatory cytokines but rather seem to be an effect of mutation-associated changes in other pathways that are not affected by treatment with canakinumab. It is conceivable that this also applies to other monogenetic autoinflammatory diseases that have a similar inflammatory phenotype and responsiveness to IL-1 inhibitors.

Despite the successful clinical response and the significant changes observed in the metabolome, this study was limited because only three family members were available for testing, which is typical in rare genetic disorders. Further studies are needed to confirm our findings and to clarify whether these results are mutation-specific or can be generalized to other known TRAPS-causing mutations or even to other known monogenic autoinflammatory fever syndromes.

Conclusion

Here we present a novel mutation in the *TNFRSF1A* gene that causes TRAPS and is associated with AA amyloidosis. Canakinumab is an effective treatment in this variant and led to improvement in proteinuria in one of the patients with presumed early renal AA amyloidosis. We observed significant changes in the metabolome compared with healthy controls affecting several pathways, most prominently arginine biosynthesis, tryptophan metabolism, and metabolism of cysteine and methionine. Treatment with canakinumab did not appear to affect these metabolic changes caused by TRAPS. Further studies are needed to examine how these pathways, which seem unaffected by treatment with canakinumab, contribute to the pathophysiology of TRAPS.

Supplementary material

Supplementary material is available at *Rheumatology* online.

Data availability

The data underlying this article will be shared on reasonable request to the corresponding author.

Funding

This work was supported by funding from the European Research Council (ERC) under the European Union's Horizon 2020 research and innovation programme (grant agreement No. 834259). J.D.S., A.Annibal, R.L. and A.Antebi were supported by the Max-Planck-Gesellschaft (MPG).

Disclosure statement: The authors have declared no conflict of interest.

Ethics: The study was conducted in accordance with the Declaration of Helsinki, and samples were collected and analyzed under protocols approved by the ethics committee (vote 12–240), University of Cologne, Cologne, Germany. The study is registered at the German Clinical Trials Registry under the ID: DRKS00010534. Informed consent was received.

Acknowledgements

We thank Nadine Hochhard and Christian Latza for technical support. The grapical abstract was created with BioRender.com.

References

1. McDermott MF, Aksentijevich I, Galon J *et al.* Germline mutations in the extracellular domains of the 55 kDa TNF receptor, TNFR1, define a family of dominantly inherited autoinflammatory syndromes. Cell 1999;97:133–44.
2. Hull KM, Drewe E, Aksentijevich I *et al.* The TNF receptor-associated periodic syndrome (TRAPS): emerging concepts of an autoinflammatory disorder. Medicine (Baltimore) 2002;81:349–68.
3. Lachmann HJ, Papa R, Gerhold K *et al.*; Paediatric Rheumatology International Trials Organisation (PRINTO), the EUROTRAPS and the Eurofever Project. The phenotype of TNF receptor-associated autoinflammatory syndrome (TRAPS) at presentation: a series of 158 cases from the Eurofever/EUROTRAPS international registry. Ann Rheum Dis 2014;73:2160–7.
4. Lainka E, Neudorf U, Lohse P *et al.* Incidence of TNFRSF1A mutations in German children: epidemiological, clinical and genetic characteristics. Rheumatology (Oxford) 2009;48:987–91.
5. Cudrici C, Deuitch N, Aksentijevich I, Revisiting TNF Receptor-Associated Periodic Syndrome (TRAPS): current perspectives. Int J Mol Sci 2020;21:3263. http://dx.doi.org/10.3390/ijms21093263.
6. Bulua AC, Simon A, Maddipati R *et al.* Mitochondrial reactive oxygen species promote production of proinflammatory cytokines and are elevated in TNFR1-associated periodic syndrome (TRAPS). J Exp Med 2011;208:519–33.
7. Simon A, Park H, Maddipati R *et al.* Concerted action of wild-type and mutant TNF receptors enhances inflammation in TNF receptor 1-associated periodic fever syndrome. Proc Natl Acad Sci USA 2010;107:9801–6.
8. Adzhubei IA, Schmidt S, Peshkin L *et al.* A method and server for predicting damaging missense mutations. Nat Methods 2010;7:248–9.
9. Choi Y, Chan AP. PROVEAN web server: a tool to predict the functional effect of amino acid substitutions and indels. Bioinformatics 2015;31:2745–7.

10. Carter PH, Scherle PA, Muckelbauer JK *et al.* Photochemically enhanced binding of small molecules to the tumor necrosis factor receptor-1 inhibits the binding of TNF-alpha. Proc Natl Acad Sci USA 2001;98:11879–84.
11. Schrödinger LaWD. The PyMOL Molecular Graphics System, Version 2.5.4. Schrödinger, LLC, 2020. https://pymol.org/2/ (3 November 2022, date last accessed).
12. Patterson RE, Ducrocq AJ, McDougall DJ, Garrett TJ, Yost RA, Comparison of blood plasma sample preparation methods for combined LC-MS lipidomics and metabolomics. J Chromatogr B Analyt Technol Biomed Life Sci 2015;1002:260–6.
13. Annibal A, Tharyan RG, Schonewolff MF *et al.* Regulation of the one carbon folate cycle as a shared metabolic signature of longevity. Nat Commun 2021;12:3486.
14. Pang Z, Zhou G, Ewald J *et al.* Using MetaboAnalyst 5.0 for LC–HRMS spectra processing, multi-omics integration and covariate adjustment of global metabolomics data. Nat Protoc 2022;17:1735–61.
15. Milhavet F, Cuisset L, Hoffman HM *et al.* The infevers autoinflammatory mutation online registry: update with new genes and functions. Hum Mutat 2008;29:803–8.
16. Van Gijn ME, Ceccherini I, Shinar Y *et al.* New workflow for classification of genetic variants' pathogenicity applied to hereditary recurrent fevers by the International Study Group for Systemic Autoinflammatory Diseases (INSAID). J Med Genet 2018;55:530–7.
17. Venselaar H, Te Beek TA, Kuipers RK, Hekkelman ML, Vriend G, Protein structure analysis of mutations causing inheritable diseases. An e-Science approach with life scientist friendly interfaces. BMC Bioinformatics 2010;11:548.
18. Nowlan ML, Drewe E, Bulsara H *et al.* Systemic cytokine levels and the effects of etanercept in TNF receptor-associated periodic syndrome (TRAPS) involving a C33Y mutation in TNFRSF1A. Rheumatology (Oxford) 2006;45:31–7.
19. Ugurlu S, Ergezen B, Egeli BH, Selvi O, Ozdogan H, Safety and efficacy of anti-interleukin-1 treatment in 40 patients, followed in a single centre, with AA amyloidosis secondary to familial Mediterranean fever. Rheumatology (Oxford) 2020;59:3892–9.
20. Negm OH, Mannsperger HA, McDermott EM *et al.* A proinflammatory signalome is constitutively activated by C33Y mutant TNF receptor 1 in TNF receptor-associated periodic syndrome (TRAPS). Eur J Immunol 2014;44:2096–110.
21. Lemos H, Huang L, Prendergast GC, Mellor AL. Immune control by amino acid catabolism during tumorigenesis and therapy. Nat Rev Cancer 2019;19:162–75.
22. Lionetto L, Ulivieri M, Capi M *et al.* Increased kynurenine-to-tryptophan ratio in the serum of patients infected with SARS-CoV2: an observational cohort study. Biochim Biophys Acta Mol Basis Dis 2021;1867:166042.
23. Sorgdrager FJH, Naudé PJW, Kema IP, Nollen EA, Deyn PP. Tryptophan metabolism in inflammaging: from biomarker to therapeutic target. Front Immunol 2019;10:2565.
24. Capuron L, Schroecksnadel S, Féart C *et al.* Chronic low-grade inflammation in elderly persons is associated with altered tryptophan and tyrosine metabolism: role in neuropsychiatric symptoms. Biol Psychiatry 2011;70:175–82.
25. Yanagawa Y, Iwabuchi K, Onoé K. Co-operative action of interleukin-10 and interferon-gamma to regulate dendritic cell functions. Immunology 2009;127:345–53.
26. Sanchez-Lopez E, Zhong Z, Stubelius A *et al.* Choline uptake and metabolism modulate macrophage IL-1β and IL-18 production. Cell Metab 2019;29:1350–62.e7.
27. Wang Z, Klipfell E, Bennett BJ *et al.* Gut flora metabolism of phosphatidylcholine promotes cardiovascular disease. Nature 2011;472:57–63.
28. Okamura DM, Pennathur S, Pasichnyk K *et al.* CD36 regulates oxidative stress and inflammation in hypercholesterolemic CKD. J Am Soc Nephrol 2009;20:495–505.
29. Cai L, Wang Z, Ji A, Meyer JM, van der Westhuyzen DR. Scavenger receptor CD36 expression contributes to adipose tissue inflammation and cell death in diet-induced obesity. PloS one 2012;7:e36785-e.
30. Coras R, Murillo-Saich JD, Guma M, Circulating pro- and anti-inflammatory metabolites and its potential role in rheumatoid arthritis pathogenesis. Cells 2020;9:827.
31. Mehta AK, Singh BP, Arora N, Gaur SN. Choline attenuates immune inflammation and suppresses oxidative stress in patients with asthma. Immunobiology 2010;215:527–34.
32. Liu L, Lu Y, Bi X *et al.* Choline ameliorates cardiovascular damage by improving vagal activity and inhibiting the inflammatory response in spontaneously hypertensive rats. Sci Rep 2017;7:42553.
33. Chiuve SE, Giovannucci EL, Hankinson SE *et al.* The association between betaine and choline intakes and the plasma concentrations of homocysteine in women. Am J Clin Nutr 2007;86:1073–81.
34. Durand P, Prost M, Loreau N, Lussier-Cacan S, Blache D. Impaired homocysteine metabolism and atherothrombotic disease. Lab Invest 2001;81:645–72.
35. Bajic Z, Sobot T, Skrbic R *et al.* Homocysteine, vitamins b6 and folic acid in experimental models of myocardial infarction and heart failure–how strong is that link? Biomolecules 2022;12:536. http://dx.doi.org/10.3390/biom12040536.
36. Townsend MH, Tellez Freitas CM, Larsen D *et al.* Hypoxanthine Guanine Phosphoribosyltransferase expression is negatively correlated with immune activity through its regulation of purine synthesis. Immunobiology 2020;225:151931.
37. Guieu R, Ruf J, Mottola G. Hyperhomocysteinemia and cardiovascular diseases. Ann Biol Clin (Paris) 2022;80:7–14.
38. Roubenoff R, Dellaripa P, Nadeau MR *et al.* Abnormal homocysteine metabolism in rheumatoid arthritis. Arthritis Rheum 1997;40:718–22.
39. Chen S, Dong Z, Cheng M *et al.* Homocysteine exaggerates microglia activation and neuroinflammation through microglia localized STAT3 overactivation following ischemic stroke. J Neuroinflamm 2017;14:187.
40. Diaz-Vivancos P, de Simone A, Kiddle G, Foyer CH. Glutathione-linking cell proliferation to oxidative stress. Free Radic Biol Med 2015;89:1154–64.
41. Torene R, Nirmala N, Obici L *et al.* Canakinumab reverses overexpression of inflammatory response genes in tumour necrosis factor receptor-associated periodic syndrome. Ann Rheum Dis 2017;76:303–9.